Statistical properties of paleomagnetic directions in Kerguelen lava flows: Implications for the late Oligocene paleomagnetic field

Pierre Camps, B. Henry, K. Nicolaysen, G. Plenier

▶ **To cite this version:**

Pierre Camps, B. Henry, K. Nicolaysen, G. Plenier. Statistical properties of paleomagnetic directions in Kerguelen lava flows: Implications for the late Oligocene paleomagnetic field. Journal of Geophysical Research, 2007, 112 (B6), pp.B06102. 10.1029/2006JB004648 . hal-00407636v1

HAL Id: hal-00407636

https://hal.science/hal-00407636v1

Submitted on 9 Mar 2010 (v1), last revised 19 Oct 2020 (v2)

HAL is a multi-disciplinary open access archive for the deposit and dissemination of scientific research documents, whether they are published or not. The documents may come from teaching and research institutions in France or abroad, or from public or private research centers.

L'archive ouverte pluridisciplinaire **HAL**, est destinée au dépôt et à la diffusion de documents scientifiques de niveau recherche, publiés ou non, émanant des établissements d'enseignement et de recherche français ou étrangers, des laboratoires publics ou privés.

Statistical properties of paleomagnetic directions in Kerguelen lava flows: implications for the Late Oligocene paleomagnetic field.*

P. Camps, B. Henry, K. Nicolaysen, and G. Plenier

Abstract

We present the results of a paleomagnetic study of seven new volcanic sections (146 flows) from Kerguelen Archipelago. For two of these sections, priliminary ($^{40}Ar/^{39}Ar$) ages are reported to aid in the calibration of the paleomagnetic results. The primary contribution of this report, however, is a compilation of these new data with those already published in order to describe statistically the characteristics of the paleomagnetic field as recorded by the Kerguelen flood basalts. In total, 258 paleomagnetic directions sampled at 13 stratigraphic sections through the lava pile are available and span an approximately 5 Myr window – from 25 to 30 Ma. The composite section represents at least 11 polarity zones that are correlated to the reference geomagnetic polarity time scale. Our approach is to investigate the average normal and reversed polarity field directions over this 5 Myr window. We calculated a paleomagnetic pole found to be located at $\lambda = 85.5^\circ$ N, $\phi = 189^\circ$ E ($A_{95} = 2.3^\circ$, K = 16.5 and N=233). This pole is in close agreement with the coeval paleomagnetic poles obtained from different worldwide places when analyzed in the Indo-Atlantic hotspot reference frame. In the statistical analysis, we tackle the specific question: is the secular variation isotropic? This question is directly related to the occurrence of a longitudinal confinement of the virtual geomagnetic poles (VGP), which is still a matter of debate amongst the paleomagnetists. By means of statistical tests, we show that the paleomagnetic data from Kerguelen agree with an isotropic model for paleosecular variation. Finally, we present adjustments to the Camps and Prevot's [1] statistical model, developed for some northern hemisphere latitudes, to the southern hemisphere paleomagnetic data from Kerguelen.

1 Introduction

During the past ten years, significant advances have been made in numerical simulation of the Earth's dynamo. Glatzmaier et al. [2] showed for the first time that a numerical model of convection-driven dynamo in spherical shells, based on the fundamental equations of the magneto-hydrodynamics and relatively realistic physicochemical properties of the Earth's core, can generate a magnetic field with a morphology and behavior close to that known for the Earth. Since then, several other numerical models were developed with the objective to be

*JGR solid Earth, 112, B06102, 2007

as close as possible to Earth-like parameters [3, 4, 5, 6]. Even if none of these models can claim to represent the geodynamo, and they will probably never be able to do so [7], they nevertheless reached a degree of improvement adding new insights to our knowledge of the Earth's deep interior. For instance, models with imposed non-uniform core-mantle boundary (CMB) heat flow [8, 9] simulate perfectly the longitudinal organization of Virtual Geomagnetic Pole (VGP), one through North and South America and the other through eastern Asia and Australia, as described by Laj et al. [10] from sedimentary records of reversals over the last 12 Myr. An alternative model that assumed a heterogeneous conducting layer at the base of the mantle [11] seems a more questionnable mechanism to influence the trajectory of VGPs during reversals [12, 13, 14].

Whatever the nature of CMB heterogeneities, the fundamental question to be addressed is inherent in the interpretation of Laj et al. [10] observations; that is, do sediments properly record rapid geomagnetic events such as reversals or excursions ? The complexity of the acquisition of remanent magnetization by sediments is such that some rock magnetists could come to the conclusion that the transitional zones observed in some sedimentary sequences are nothing more than artifacts [15, 16]. In contrast, volcanic rocks are reliable recorders of the geomagnetic field. However, statistical analysis of the location of transitional VGPs recorded exclusively by volcanic rocks from all around the world during the last 20 Myr, have proposed conflicting conclusions [17, 18, 19].

Examination of paleosecular variation (PSV) provides an alternative source of information into the possible control of the configuration of the paleomagnetic field by the lower mantle. Constable [20] pointed out that one of the preferred longitudinal bands coincides with that expected from reversal of a non-axial dipole field exactly like that present in the modern day field. Then, she argued that if persistent non-zonal terms exist, they may generate VGP positions non-uniformly distributed in longitude even during times of stable polarity, as seems to be supported by the global PSV volcanic records for the last 5 Myr [20]. On the contrary, Camps and Prevot [1] showed that the PSV remains isotropic during the last 15 Myr at the regional scale of Iceland. Thus, despite the large number of paleomagnetic studies devoted over the past 20 years to the study of the geomagnetic field fluctuations – from PSV to reversals – the question of whether the lower mantle influences the core dynamo is still a matter of debate.

We believe that useful input to this issue may be obtained by studying the statistical properties of the field fluctuation over several Myr at a particular region, similar to previous studies of Iceland [21, 1]. The French volcanic islands near Antarctica – New Amsterdam, Crozet and Kerguelen Archipelagos – located in the southern Indian Ocean represent an uncommon opportunity to carry out such a regional study. The sub-aerial volcanism is of different ages in these islands; younger than 1 Ma in Amsterdam, Plio-Pleistocene in Crozet and mainly Oligocene in Kerguelen. Recent paleomagnetic results obtained from this area deserve special attention. First, PSV data for the last 5 Myr recorded in lava flows from Possession Island (Crozet Archipelago) [22] agree with the general anisotropic PSV model proposed by Constable et al. [23], which assumes that the boundary conditions at the core-mantle interface are geographically heterogeneous. Second, the transitional field of two distinct recent excursions, one recorded in Possession Island [22] and the other recorded in Amsterdam Island [24], located 2300 km northeast-ward from Crozet Archipelago, each would have revisited the same VGP location, which is within one of the preferred longitudi-

nal bands of Laj et al [10]. Both of these observations support the controversial hypothesis of mantle influence on the dynamic of the outer core. Those seem however to be limited to the few last Myr because the PSV data obtained on Kerguelen, a volcanic archipelago located in the same part of the southern Indian Ocean for which the sub-aerial flows are mainly of Late Oligocene age, agree with an isotropic model for PSV [25].

We propose in the present study to address further the statistical description of the paleomagnetic field fluctuations recorded on Kerguelen by reporting 146 new paleodirection determinations to supplement previous studies [26, 25] and then proposing a statistical model for the paleomagnetic field fluctuations compatible with the whole dataset (258 paleodirections).

2 Paleomagnetic sampling

A statistical description of the paleofield fluctuations imposes some constraints on the way in which sampling must be carried out. For instance, it has to be homogeneous over a period of time as long as possible. To accomplish this, our field work strategy dictated that we avoid significant temporal overlap between the different stratigraphic sections while taking care to leave a minimum of time intervals unsampled. For each section, we decided to sample each successive lava flow even if this choice is questionable and time-consuming. On one hand, the Camps and Prevot [1] model requires inclusion of the full spectrum of field fluctuations, from secular variation to reversals, hence, we want to recover any existing magnetic transitional directions. Moreover, due to the particular field trip conditions encountered on Kerguelen – difficulty and cost of accessing the archipelago combined with logistically field conditions – the possibility to supplement later a sampling is always uncertain. On the other hand, in the absence of very accurate age estimate for each flow and due to the episodicity of volcanism, only the chronological order is known for the instantaneous records of the paleomagnetic field provided by a succession of lava flows, not the time elapsed between each flow and its captured reading of the magnetic field. Thus we have to assume, tentatively, that each flow represents an independent reading of the geomagnetic field which is not true if several successive flows are erupted in a short time interval.

We benefited from a very detailed geological knowledge of the Archipelago [27], intensive stratigraphic geochemical investigations (see Doucet et al [28] for a review) and numerous radiochronologic ages [29, 30, 31] to make an initial selection of the sampling sites. Then, we kept only those not affected by significant tectonic events and presumed to encompass a large time interval, e.g., recovering a maximum number of minimally altered lava flows.

Paleomagnetic studies of the volcanic sequences very often come up against the difficulty to know if, when the lavas in the section show a small dip, this dip is of tectonic or topographic origin. In the present case, our choice whether to apply a tectonic correction was determined from geological data [27], our own field observations and partly from studies of the magnetic fabric [32, 33] that can make it possible in certain cases to find the flow direction of the lava. We did not apply corrections when the flow direction and the azimuth of the present dip are similar, because we cannot exclude the hypothesis that this one is of topographic origin and inherent to the flow. The contrary case, i.e., dip

direction and flow direction are not the same, indicates without any doubt that a post-emplacement tilting occurs, and thus it was taken into account.

Seven new cross-sections supplementing the former studies are presented below and located on Figure 1. Additional informations may also be retrieved from an electronic supplement (Table A1).[1]

1. **Port Jeanne d'Arc** : We continued the previous paleomagnetic sampling of Henry et al [26] at the Ravin du Charbon starting at the next flow upward and sampled also a second section at Ravin Jaune, 2 km east from Ravin du Charbon, where additional flows crop out stratigraphically beneath those of the former published sampling. Interbedded conglomerate deposits overlain by trachytic tuffs and breccias provide obvious stratigraphic correlations between theses two sections. Eruption of these lava are interpreted from $^{40}Ar/Ar^{39}$ dating to be synchronous at 25 Ma [29]. We present 25 paleomagnetic directions in a combined section of 400 m of cumulative thickness. These directions have been corrected from a gentle post-emplacement tilting, 5 $^\circ$ towards the WNW, as recommended by Henry et al [32].

2. **Ile Haute** : We sampled 22 lava flows through a 320 m thick vertical cross-section. This site was selected because in a previous paleomagnetic study, Derde et al [34] have suggested the presence of intermediate field directions. No radiochronological age is available as the plagioclase feldspar and glassy groundmass, upon which the argon dating relies, have begun alteration to clays. In this area, lava flows present a constant and very gentle dip of 2 $^\circ$ toward the East. However, we did not correct for tilting the paleomagnetic directions obtained in this section since this dip is similar to the flow direction inferred from field observations [27], and thus it is certainly of topographic origin.

3. **Port Raymond** : We selected this 250 m thick vertical cross-section because there is no doubt from field observations that it corresponds to the direct downward continuity of the Ile Haute section with little or no overlap. Nine lava flows have been sampled. Plenier et al [33] confirmed from AMS measurements that the flow direction is eastward, e.g., similar to the present dip. Thus the data for this section was not corrected for tilting.

4. **Mont Bureau** : Watkins et al [35] reported a paleomagnetic study carried out on the 7 lower flows, but these directions should be regarded with caution as attested by the large values of the 95% confidence limits for the mean direction α_{95}. We re-sampled exactly the same flows plus 11 overlying flows. The thickness of our section is about 400 m. We recommend that our results do not complete but instead supersede the ones described by Watkins et al [35]. This lava pile was emplaced between 29.3 Ma and 28.5 Ma [30]. Yang et al [36] did not find obvious evidences from petrographic observations and geochemical analysis to constrain stratigraphic correlation between this section and the coeval Mont Rabouillère section [25]. Again, we did not apply corrections for a post-emplacement tilting

[1] Auxiliary material is available at ftp://ftp.agu.org/apend/jb/2006JB004648

since the very gentle dip of 2 ° towards the NE, that we directly measured, seems to correspond to the flow direction [33].

5. **Port Christmas** : 16 flows have been subject to a paleomagnetic sampling. Unfortunately, owing to very difficult field working conditions, we had to stop sampling before reaching the top of this section, leaving about 10 flows unsampled. An argon isotopic study failed to give reliable ages, probably due to a significant post-magmatic alteration. Lava flows are sub-horizontal.

6. **Trois Ménestrels** : To date, neither paleomagnetic nor geochemical studies have been carried out on volcanic rocks from this wide area located in the Southern part of the Archipelago. We sampled 42 lava flows through a 650 m thick section. A preliminary Ar/Ar date for the top of the section is presented below, and a geochemical study of this section is in progress (H. Diop, personal communication). Directions have been corrected for a tectonic post-emplacement tilting (dip = 8 ° and dip direction = 120 °) estimated from field measurements of several apparent dips. This correction seems to be justified since the present dip significantly differs from the flow direction assumed to be southward in this area [27].

7. **Sentinelles** : Located just few km south of Trois Menestrels, we suspected from field observations that this section partly overlaps the Trois Menestrels. Thus, only 14 ~~flows~~ volcanic units were sampled to from a 160 m cumulative thickness. Preliminary Ar/Ar dates for the top and base of the section are presented below. Directions were transformed into tilt adjusted coordinates (dip = 8 ° , dip direction = 103 °). This correction is estimated, as for the Trois Menestrels section, from field measurements of several apparent dips.

For each section the sampling was carried out identically. We collected an average of seven cores for each successive flow using a gasoline-powered portable drill. Samples were oriented using a magnetic compass corrected for local and regional anomaly by sighting either the sun at a known time or known landmarks.

3 Paleodirection determinations

We determined the paleodirections according to a standard procedure adopted in our laboratory. It consists in treating two pilot samples from each flow in a null magnetic field environment, one by stepwise alternating fields (AF) and a second by stepwise heatings, using a very detailed experimental procedure involving up to 18 steps. Assuming that the remanence properties are homogeneous at a flow scale, the remaining samples for each flow are then treated with a reduced number of selected steps – between 7 and 10 – according to the paleomagnetic treatment which seems to us the best adapted to isolate the Characteristic Remanent Magnetization (ChRM). Examples of demagnetization diagram for normal, reverse, and intermediate polarity are presented in Figure 2. We determined ChRM directions by means of the principal component analysis using the Maximum Angular Deviation (MAD) [37] as a measure of the inherent

scatter in directions. We averaged the directions thus obtained by flow, and calculated the statistical parameters assuming a Fisherian distribution [38]. The complete results of these analysis are given in Table A1. The ChRM directions cluster well for each flow with rather small values of the 95 % confidence limits about the mean direction (α_{95}), 45% of determinations are $\leq 5^\circ$ and 96% $\leq 10^\circ$.

4 Additional $^{40}Ar/^{39}Ar$ age determinations

Three samples were chosen for dating from Trois Menestrels and Sentinelles sections such that the greatest possible stratigraphic range was obtained and that the samples showed the least post-emplacement alteration. K2S-1, K2S-17 and K2M-59 come respectively from the bottom and top of the sampled Sentinelles section and the top of the Trois Menestrels section. Unfortunately the four lowermost flows from the Trois Menestrels section showed significant alteration including calcite veins and abundant chlorite in the groundmass. The three dated samples contain microphenocrysts of plagioclase, clinopyroxene and abundant iron-titanium oxides and have a nearly holocrystalline matrix. Vesicles are filled with chlorite and the olivine phenocrysts of KSM-59 have similarly altered to chlorite and other clays.

The samples were crushed and sieved to obtain 0.3-1.0 mm size fractions, which were then hand-picked to obtain a uniform whole rock separate that was sent to the Nevada Isotope Geochronology Laboratory (NIGL) at the University of Nevada, Las Vegas. After a final picking at NIGL, samples were packaged with Fish Canyon Tuff sanidine and CaF_2 and K-rich glass fluence monitors followed by irradiation for 7 hours at the McMaster University Nuclear Reactor in Ontario. Fusion of 3-5 crystals of the fluence monitors yielded J-values whose reproducibility was 0.05-0.35% throughout the 100 mm long irradiation package and the neutron flux varied less than 4%. Other corrections factors include: $(^{40}Ar/^{39}Ar)_K = 0.0001 \pm 100\%$, $(^{36}Ar/^{37}Ar)_{Ca} = 2.62(\pm 2.28\%).10^{-4}$ and $(^{39}Ar/^{37}Ar)_{Ca} = 6.59(\pm 0.44\%).10^{-4}$. At NIGL standard laser and furnace step-heating procedures were used (see Appendix B of Reiner et al [39]) and during these analyses $^{40}Ar/^{36}Ar = 291.24 \pm 0.24\%$; thus a mass discrimination correction of 1.01400 was applied to the data, which were reduced and ages were calculated using LabSPEC software (B. Idleman, Lehigh University). During the data reduction at NIGL, the Fish Canyon sanidine was assigned an age of 27.9 Ma [40, 41], but the data were recalculated using an age of 28.02 Ma for the standard so that these results may be compared consistently with those of previous studies [30].

Each of the samples resulted in a total gas age, considered equivalent to a K-Ar age (Table A2)[1]. Neither isochron nor plateau ages, as defined by McDougall [42] and Wendt et al [43], were obtained within the 1σ confidence limits. Although plateaus were not obtained, the age spectra do not show evidence of partial diffusive loss. The ages obtained for K2S-1 (28.95±0.22Ma) and K2S-17 (27.02 ± 0.14 Ma) are consistent with the stratigraphy; that is, the age of the base of the section is older. K2M-59, the top of the Trois Menestrels section yields an age (27.84 ± 0.12 Ma) that overlaps with the range of the Sentinelles section. These ages are younger than those measured on basalts exposed on the northern and northeast peninsulas of the archipelago (∼29 Ma)

but significantly older than those of the sections sampled at Mt. Crozier and at the Jeanne d'Arc peninsula (∼25 Ma) [29, 30, 31].

5 The Kerguelen paleomagnetic dataset

We gathered the data described in the present study with those previously published by Plenier et al [25] and Heny et al [26]. We did not include in this new dataset the sections of Port Douzième and Puy Saint-Théodule [26] because their ages are unknown, and the Grande Cascade section [35] because the latter was partly re-sampled last year in order to determine its age and better specify some paleomagnetic directions. This study is still on progress. On the whole we collected 258 directions sampled at 13 sections through the lava pile. This sampling represents about 4000 m of cumulative thickness of Kerguelen flood basalts.

5.1 Stratigraphic correlations

We think important in a statistical analysis of the paleomagnetic field fluctuations to have an elementary knowledge of the temporal succession of field recording. Here, this is achieved by tentatively correlating the measured Kerguelen polarity zones to the Oligocene Geomagnetic Polarity Time Scale (GPTS), using the same working hypothesis as Plenier et al [25]. Firstly, they assumed that all the polarity chrons spanning the emplacement of a section were recorded. Secondly, when ages within the 2σ uncertainty do not allow an unique interpretation, they kept the solution closest to the best available age. In this exercise, it is important to keep in mind, as underlined by Riisager et al [44], that there are also uncertainties on the GPTS ages. We chose arbitrarily to refer to the Huestis and Acton [45]'s GPTS rather than that of Cande and Kent [46]. These two GPTS calculated from different magnetic anomalies differ from 0.260 Ma to the maximum during the Late Oligocene which is not really significant for our purpose. To be accurate, we adjusted Huestis and Acton [45]'s GPTS +0.6% downward in age in accordance with the revision of the Fish Canyon sanidine reference standard (28.02 Ma) used for Kerguelen Ar isotopic studies [30] whereas the reported GPTS used the old value (27.84 Ma).

Hence, the R-N transition recorded at Port Jeanne d'Arc would coincide with the termination of the chron C7n-1r. Without a doubt, the Trois Ménestrels section spans an interval during the C9n chron, and Mont Bureau section would partly overlap the Mont Rabouillère section during the chrons C10r and C10n-2n (Figure 3). Among the sections for which at least one isotopic age is available, only the Mont de la Tourmente section poses a problem of correlation already widely discussed by Plenier et al [25]. They had no basis to clearly assign this section to a specific chron, as four possibilities were statistically acceptable. Of course, the correlation of the sections for which we do not have an absolute age is clearly more dubious. We have, however, important reasons to think, according to our field observations and local geology knowledge, that the combined section Ile Haute/Port Raymond is stratigraphically located just under the Mont Amery section. For the same reasons, we think that Port Couvreux section is just below Port Raymond. The stratigraphic correlation of Port Christmas section is also uncertain. From geological considerations, flood basalts in this area

are presumed to have erupted around 28 Ma [A. Giret, personal communication], which leaves us few possibilities of correlations since 3 polarity chrons are present in this section. Our preferred interpretation is to consider this section coeval to the chrons C10n-1n, C9r and C9n. Unfortunately, it is not easy to compare volcanic data from different sites, even when they can be demonstrated to correspond to the same reversal or the same polarity zone.

We believe that although some sections have the same age, the distance between the sections and paleotopographic controls on flow emplacement preclude the possibility that the exact flow sequence was sampled several times at different locations. They usually provide complementary paleomagnetic records. This could explain why, for all of these sections, we could not strengthen the proposed correlations using paleomagnetic direction.

To summarize, we believe that the Kerguelen dataset would cover at least 11 polarity zones of the 16 known for the Late Oligocene, from 25 to 30 Ma (Figure 3).

5.2 The Kerguelen paleomagnetic pole

By definition, a paleomagnetic pole has to be calculated from data that are representative of the axial dipole model. There are no doubts that the Kerguelen sampling, which encompass 5 Ma of field fluctuation recording, is well suited to calculate a paleomagnetic pole with the condition that we can isolate the transitional data. This problem is not as simple as one could think. There is presently no general agreement regarding the upper limit of paleosecular variation (PSV). Most commonly, VGP latitudes in the geographical reference frame, rather than local field directions, are used to delimit the PSV realm. The proposed threshold to avoid inclusion of transitional data varies between a maximum of 60° [17] and a minimum of 35° [21], a 45° value being often used for the calculation of the VGP scatter representative of paleosecular variation [47]. Vandamme [48] speculated that since the PSV depends on the site latitude, the VGP cutoff should also be latitudinally dependent. Then, he proposed a numerical procedure to calculate an optimum cutoff angle based on the assumption that a given VGP distribution is described by the sum of two contributions : a Fisherian distribution for the PSV and an uniform distribution for the transitional regime. The main drawback is that the PSV subset selected in this procedure has to be Fisherian and thus has azimuthal symmetry about the mean, which is one of the statistical characteristics we want to investigate. As a result of this uncertainty on the VGP cutoff, estimate of the paleomagnetic pole position and figures calculated for describing the dispersion ascribed to PSV are somewhat arbitrary. Paleosecular variation in Kerguelen is of little interest until compared with a global model for the same time interval. Unfortunately, many statistical models for paleosecular variation, such as the most recent one TK03 [49], are constructed to fit the paleomagnetic data for the last 5 Ma. To our knowledge, only one PSV model exists for the Oligocene data [47], which is fitted using a dataset limited to the VGPs having a paleolatitude greater than $\pm\ 45^\circ$. Thus in the present analysis, the VGP cutoff is necessarily the same.

Now one other difficulty exists : the geographical reference frame is estimated back through time only from mean global paleomagnetic poles that depend on models of the relative positions of tectonic plates. To overcome this difficulty, we will assume that the mean Kerguelen pole is representative on the paleogeo-

graphic axis, and thus we consider VGPs having a latitude less than $\pm 45^\circ$ in the Kerguelen mean pole reference frame as transitional. We calculated the mean paleomagnetic axis from an iterative eigenvector analysis, starting with all poles and removing step by step the furthest VGP until all VGPs were located at an angular distance from the mean axis lower or equal to 45°. In total, we excluded from the analysis 25 VGPs considered to be ~~transitional~~ intermediate, e.g., indicating either a polarity reversal or a geomagnetic excursion.

VGPs locations have been analyzed for both normal and reversed polarities (Table 7) in the present geographical reference frame. The angle between the mean VGPs of normal and reversed polarities is 177.3°. That is, when one of the mean poles is flipped to its antipode, each mean poles lies inside the 95% confidence region of the other. The reversal test is necessarily positive. This conclusion is illustrated graphically (Figure 4) by means of the bootstrap test for a common mean [50] and furthermore validated with a formal statistical test [51]; the angle of 2.7° found between the two mean poles being less than the critical angle of 4.8°. A positive reversal test ensures that the paleomagnetic treatment removed successfully the secondary NRM, and that the sampling averaged adequately the PSV. We processed the combined data by reversing the VGPs of reversed polarity to calculate a paleomagnetic pole found at 85.5°N, 189.3°E in the present latitude-longitude grid. This location is estimated with a very good statistical precision as attested by the low value of A_{95}, 2.3°. We deduced from this paleomagnetic result that the Kerguelen Archipelago latitude at the Late Oligocene was about 51°S, eg less than 2° south of its present location. Finally, we point out that this new Kerguelen paleomagnetic pole is in perfect agreement, within 2°, with the master apparent polar wander path for the Antarctica plate [52].

5.3 The global Late Oligocene paleomagnetic pole

An additional test for the reliability of the Kerguelen paleomagnetic pole is to check whether this pole is in close agreement with the coeval paleomagnetic poles obtained from different locations worldwide. Eight poles (Table 7), for which the estimated ages within error falls in the interval 25-30 Ma, have been selected using the same selection criteria as in Prevot et al [53]. That is, the selected poles are restricted to magmatic units, calculated from a minimum of 10 sites with at least 5 samples per sites, and must have an associated Fisher dispersion parameter K between 10 and 100. Larger K are generally indicative of an inadequate sampling of PSV. We performed this comparison in the Indo-Atlantic hotspot reference frame. The finite rotation poles used to transfer the paleomagnetic poles into this new reference frame are calculated from Royer et al [54] and Muller et al [55]'s reconstructions using a global circuit through Central Africa. We used the mean age associated with each paleomagnetic pole to calculate the finite rotation (Table 7) assuming a linear interpolation with time between the total reconstruction poles yielded in the literature at 20.5 and 35.5 Ma.

In the Indo-Atlantic hotspot reference frame, the Kerguelen paleomagnetic pole is located within the 95 per cent confidence cone about the mean global Late Oligocene pole (86.4°N, 160.1°E, $A_{95}=4.6^\circ$, K = 146.9, N=8) (Figure 5). We conclude that this pole should be considered as very reliable and thus can be combined with the 8 others. The mean Late Oligocene paleomagnetic pole

is then estimated at (86.4 ° N, 162.6 ° E, A_{95}=4.0 ° , K = 166.6, N=9) ,e.g., at about ∼4 ° from the Earth's actual spin axis. Prevot et al [53] and Besse et al [52] have already observed this 4 ° difference, but their interpretations differ. In Prevot et al [53] this difference is explained as "secular" wandering, induced by some transient modifications of the inertia tensor of the Earth, of the instantaneous geographic pole around its time-averaged position, whereas Besse et al [52] proposed a change in the time-averaged position of the rotation axis, what is literally called true polar wander (TPW). A controversial debate exists on TPW; some authors consider that TPW as seen from the paleomagnetic data is purely an artifact [56]. Then, a further discussion on the explanation of the difference between the global oligocene pole calculated in the present study and the actual Earth's spin axis is beyond the scope of the present study.

5.4 The Late Oligocene mean magnetic field

In the preceding discussion, we assumed that the time-averaged field is purely dipolar. We propose now to check whether the averaged field during the Late Oligocene includes a significant zonal quadrupolar component (g_2^0) as it was suggested by Rochette et al [57] but not confirmed in Riisager et al [44]'s analysis. We performed the test by calculating the local field directions from the 9 selected poles and then recalculated each pole location assuming various contributions of an axial quadrupole component. In practice, we used the offset dipole model [58] in which the local field inclination (I) is related to the paleomagnetic colatitude (θ) by :

$$I = \tan^{-1}\left[2\cot\left\{\theta\sin^{-1}\left(\frac{x\sin\theta}{\rho}\right)\right\}\right] - \sin^{-1}\left(\frac{x\sin\theta}{\rho}\right)$$

where $\rho = (x^2 + R^2 - 2Rx\cos\theta)^{1/2}$, R is the radius of the Earth and x, the displacement positive northward of the dipole along the rotational axis. This displacement can be expressed in term of harmonic coefficients by :

$$x = \frac{1}{2}\frac{g_2^0}{g_1^0}R$$

The test consists of searching for, through an iterative process, the value of the dipole displacement that produces the minimum scatter in the 9 poles when analyzed in the hotspot reference frame. We found that the best grouping is obtained when the quadrupole/dipole field ratio is between 3 and 4% (Figure 6), a value similar to the one suggested by paleomagnetic data obtained from volcanic rocks less than 5 Ma old [59, 60]. In order to validate this observation further, we repeated the same test nine times, removing in turn one pole at each run. Regardless of the 8 poles-subset used, the best grouping is always found for a small positive quadrupole/dipole field ratio, between 2 and 5 % (Figure 6).

5.5 The paleosecular variation regime

It is noteworthy to recall first that by defining the PSV domain by means of a VGP cutoff precludes any statistical study of the paleomagnetic fluctuations on the local field direction reference frame. Indeed, as expected from geometrical

considerations, the PSV domain is significantly off-center with respect to the mode of the distribution of the local field direction as illustrated on Figure 7.

The quantity of principal interest in PSV study is the between site angular standard deviation (asd) S_B which is calculated from the total asd S_T corrected for experimental error by removing the within-flow asd S_W:

$$S_B^2 = S_T^2 - \frac{S_W^2}{\overline{n}}$$

with

$$S_T = (N-1)^{-\frac{1}{2}} (\sum_{i=1}^{N} \delta_i^2)^{\frac{1}{2}}$$

and

$$S_W \approx \frac{81^\circ}{\sqrt{\overline{k}}}$$

where N is the number of data, δ_i the angle between the ith VGP and the reference position, $\overline{n}$ is the mean number of samples per unit, and $\overline{k}$ the mean precision parameter. Results of these calculations are reported in Table 7. The value of S_B is almost exactly the value of 20.9° predicted by the PSV model of McFadden et al [47] for the given age and paleolatitude. Of course, this result substantiates the model hypothesis among which two are worth noting : the PSV is assumed to be isotropic about the Earth's spin axis, e.g. latitudinal dependent only, and symmetric about the equator. Moreover, it gives additional arguments to think that the PSV has been sufficiently and properly sampled in the present study.

5.6 Azimuthal symmetry

As mentioned above, the azimuthal symmetry of VGP longitude distribution is one of the most controversial debates among the paleomagnetists. Usually, authors give an initial qualitative estimate of their azimuthal distribution by means of graphical diagrams such as simple circular histograms or rose diagrams of VGP longitudes [20, 17, 19]. However, most of these diagrams involve an arbitrary choice of both the origin and the width of intervals, which can significantly distort the information if they are inappropriately chosen. That is not the case with the kernel density estimate diagram [61] as used in the present study. In this method, the density estimate in a given longitude ϕ ($0 \leq \phi \leq 2\pi$) is :

$$\hat{f}(\phi) = \frac{1}{nh} \sum_{i=1}^{n} w\left(\frac{\phi - \phi_i}{h}\right)$$

where n is the number of data, h a smoothing factor and w a quartic kernel function such as :

$$w = \begin{cases} 0.9375(1-\phi^2)^2 & : \quad -1 \leq \phi \leq 1 \\ 0 & : \quad \text{otherwise} \end{cases}$$

The density estimate function was computed using the algorithm given in Fisher [61].

There is no obvious visual evidence either for a major modal group or for two antipodal groups in the Kerguelen VGP longitudes distribution (Figure 8). Several small bumps suggest rather an azimuthal symmetry about the mean VGP. These considerations can be made much more precisely and quantitatively with formal statistical tests of hypothesis. First, we checked the hypothesis of uniformity for Kerguelen VGP longitudes against all possible alternative distributions by means of the Kuiper's statistic [61], a Kolmogorov-type test that does not depend on the choice of the zero direction. The criterion for the Kuiper's statistic is :

$$V_n = \max(U_i - i/n) - \min(U_i - i/n) + 1/n$$

where $U_i = \phi_i/2\pi$ for each VGP longitude ϕ_i as arranged in numerical order, n being the number of data. Provided n is large in the present case, we can calculate the modified Kuiper's statistic :

$$V_n^* = (n^{\frac{1}{2}} + 0.155 + 0.24n^{-\frac{1}{2}})V_n$$

which is compared with the critical values given in Table 7.1 of Mardia [62]. Results are given in Table 7 for several data subsets. The hypothesis of uniformity for VGP longitude is strongly rejected when the VGPs are analyzed in the present geographical reference frame, and there is no evidence for a departure from an uniform distribution when VGPs are rotated into the mean pole reference frame both for the PSV dataset (N = 233) and the whole dataset (N = 258). These results call for several comments. First, given that the mean pole location is different from the geographic axis, if a rotational symmetry about the mean pole is observed, it is only normal that a bias toward the mean pole longitude exists when the test is performed in the geographical reference frame. To illustrate this, we calculated the mean longitude $\bar{\phi}$ in the geographical reference frame of the vector resultant of $\phi_1, \ldots, \phi_n$ for the PSV dataset :

$$\bar{\phi} = \tan^{-1}(\sum_{i=1}^{n} \sin\phi_i / \sum_{i=1}^{n} \cos\phi_i)$$

and found 181.2 $^\circ$ which is close to 189.3 $^\circ$, the mean pole longitude (Table 7). We believe it important to keep this point in mind when such analyses are performed. Next, as the difference between the mean pole and the geographic axis is small in the present case (4.5 $^\circ$), the different answers for the Kuiper test can be seen as proof of its strength, and thus its use is even more justified.

Finally, to assess this discussion, we can look into the more precise question of whether the Kerguelen dataset could be consistent with the longitudinal organization of VGP within two antipodal preferred bands. The Rayleigh test is perfectly adapted for this purpose if we transform each VGP longitude ϕ_i to ϕ_i' by :

$$\phi_i' = (2\phi_i)(\mathrm{mod}2\pi)$$

and treat ϕ_i' as observations from an unimodal distribution for which the mean longitude is unknown. In this case, the criterion of the Rayleigh test is $\bar{R}$, the mean resultant length associated with the mean longitude $\bar{\phi'}$ [61] :

$$\bar{R} = \frac{1}{n}\sqrt{\left(\sum_{i=1}^{n}\cos\phi_i'\right)^2 + \left(\sum_{i=1}^{n}\sin\phi_i'\right)^2}$$

To find the critical values, we allowed the approximation for large n that $2n\bar{R}^2$ is distributed as $\simeq \chi^2_2$ [62]. The results are a little more ambiguous than for the Kuiper test (Table 7). We found in this analysis of the PSV dataset a little evidence to suggest a departure from the model of uniformity when tested against a bimodal distribution, however the significance level is only $\simeq 3.7\%$ found using the table given in appendix A.2b of Fisher [61] . On the other hand, we have no evidence to reject the hypothesis of azimuthal symmetry about the mean when the whole dataset (N=258) is considered.

5.7 Statistical modeling

In this last section, we adapt the Camps and Prevot [1]'s statistical model, developed for some northern hemisphere latitudes, to the paleomagnetic data from Kerguelen. This model considers the paleomagnetic local field vector to be the sum of two independent set of vectors : the secular variation vector set (SV) characterized by an uniform orientation and a magnitude defined by a Maxwell-Boltzmann probability density function (pdf), and the axial vector set (AD) characterized by a constant direction and magnitude defined by a non-zero mean gaussian pdf $\mathrm{N}_{AD}(\mu, \sigma^2)$. In practice, the SV vectors are generated from their cartesian coordinates which are distributed as three independent random gaussian variables having the same $\mathrm{N}_{SV}(0, \sigma^2)$ distribution. By means of a Monte Carlo simulation, a large number of local field vectors are generated, 20000 in the present case, and then transformed to VGP with their associated Virtual Dipole Moment to be compared with the experimental data.

In term of harmonic coefficients, the axial vector set corresponds to an axial dipole plus a small axial quadrupole, both reversing simultaneously. According to theoretical inferences [63], the fundamental assumption in this model is that there is no transfer of the AD energy into other harmonic coefficients, even when the AD decreases to zero. Camps and Prevot [1]'s showed that a correct statistical model requires a statistically representative sampling of the full spectrum of field fluctuations, from secular variation to reversals, and both directional and intensity analysis. From this point of view, the volcanism in Kerguelen is especially interesting because it encompass 5 Ma and because three transitions and several excursions seem to be documented (Table A1). Unfortunately, only a few absolute paleointensity determinations exist [64] and the average remanence intensities cannot be used as a proxy due to the presence of various secondary remanent magnetizations observed in Kerguelen lavas.

We determined the model parameters by keeping the same fluctuation for the AD vector as the one determined for the Icelandic data set [1] and by matching the SV fluctuation only to the VGP co-latitude data (Figure 9). We found that the 258 Kerguelen VGP co-latitudes are well simulated with the model parameters $\mathrm{N}_{AD}(\mu = 1, \sigma^2 = 0.2)$ and $\mathrm{N}_{SV}(\mu = 0, \sigma^2 = 0.029)$. The secular variation appears to be latitudinally dependent and decreases with the site latitude if compared to the value found for the Icelandic data set $\mathrm{N}_{SV}(\mu = 0, \sigma^2 = 0.04)$ [1]. We highlight this observation as it is a characteristic commonly reported in PSV models (see, e.g.,McFadden et al [47]), however we must be very careful with further interpretation. Our modeling is not as precise as if we had been able to use the paleointensity as a constraint and above all it is very speculative to compare statistical properties of data of different ages, i.e., the Icelandic data is of Miocene age.

6 Conclusions

Thanks to the 146 news data reported in this paper combined with data from two previous studies [26, 25], we gathered a data set of 258 paleomagnetic field directions as recorded by basaltic lava flows from the Kerguelen Archipelago. From magnetostratigraphic correlations and absolute Ar/Ar radiometric ages, we showed that these data represent a rather homogeneous sampling of the paleomagnetic field fluctuations through the last 5 Ma of the Oligocene. A positive reversal test of class A [51] guarantees further that the sampling adequately averages the PSV during both polarity intervals. Thus, we believe that the Kerguelen data set is particularly well suited to describe the characteristics of time-averaged paleomagnetic field and those of the PSV as observed from this part of the southern Indian Ocean between 25 and 30 Ma. From these considerations, we have shown that :

1. There is no statistically significant difference between the Late Oligocene time-averaged normal and reverse polarity as shown by a common mean and a common concentration parameter κ (Table 7).

2. The Kerguelen paleomagnetic pole, $\lambda = 85.5\,^{\circ}$N, $\phi = 189.3\,^{\circ}$E, $A_{95} = 2.3\,^{\circ}$, K = 16.5, in the present latitude-longitude grid, should be considered very reliably determined. In addition to the arguments cited above, this conclusion is strengthened by the close agreement observed between the Kerguelen paleomagnetic pole and the mean pole calculated for the master apparent polar wander path for the Antarctica plate [52]. Very good agreement is also observed when we compare this pole in the Indo-Atlantic hotspot reference frame with a selection of 8 contemporaneous paleomagnetic poles obtained from different worldwide locations.

3. The time-averaged Oligocene paleomagnetic field is rather compatible with a model of an axial dipole plus a small zonal quadrupole (4% of the dipole value), both reversing simultaneously.

4. The azimuthal symmetry of the VGP distribution about the paleomagnetic pole, observed for the PSV and the whole dataset, does not support the presence of persistent non-zonal terms in the time-averaged field over the period 25-30 Ma. This conclusion, also corroborated by the perfect agreement between the Kerguelen VGP scatter and the McFadden et al [47]'s PSV model, is at variance with younger records of the paleomagnetic field fluctuations obtained from the same area in Crozet Archipelago [22] and Amsterdam Island [24]. Thus, persistent non-zonal terms, which can be viewed as proxy for the effect on the core dynamo of spatially heterogeneous core-mantle boundary conditions, seems to be limited to the last few Ma as suggested by the data from the southern Indian Ocean. However, this conclusion conflicts with a recent claim by Hoffman et al [65] who conclude for a longer time constant – at least 25 Ma – for the control by the lower-most mantle on the configuration of the paleomagnetic field from a detailed description of a polarity change recorded in a continuous sequence of lava flows in southeastern Queensland, Australia.

7 acknowledgments

We are grateful to the "Institut Polaire Paul Emile Victor" for providing all transport facilities and for the support of this project. Special thanks to Alain Lamalle, Roland Pagni and all our field friends. We thanks Michel Prévot for scientific discussions, Thierry Poidras and Patrick Nicol for technical help during laboratory experiments. KN thanks Kathleen Zanetti and Terry Spell for analyzing the argon aliquots at University of Neveda, Las Vegas. Further support for KN was provided by a grant to Dr Dominique Weis at ULB and the argon dates themselves were funded by Kansas State University research grant awarded to KN. Reviews by Pierrick Roperch and Lisa Tauxe helped to clarify several issues and are much appreciated.

References

[1] P. Camps and M. Prévot. A statistical model of the fluctuations in the geomagnetic field from paleosecular variation to reversal. Sciences, 273:776–779, 1996.

[2] G.A Glatzmaier and P.H. Roberts. A three-dimensional convective dynamo solution with rotating and finitely conducting inner core and mantle. Phys. Earth Planet. Int., 91:63–75, 1995.

[3] W. Kuang and J. Bloxham. An Earth-like numerical dynamo model. Nature, 389(6649):371–374, 1997.

[4] P. Olson, U. Christensen, and G.A. Glaztmaier. Numerical modeling of the geodynamo: Mechanisms of field generation and equilibration. J. Geophys. Res., 104:10383–10404, 1999.

[5] A. Sakuraba and M. Kono. Effect of the inner core on the numerical solution of the magnetohydrodynamic dynamo. Phys. Earth Planet. Int., 111:105–121, 1999.

[6] F. Takahashi, M. Matsushima, and Y. Honkura. Simulations of a quasi-taylor state geomagnetic field including polarity reversals on the earth simulator. Science, 309(5733):459–461, 2005.

[7] R. Holme. A fuel-efficient geodynamo? Nature, 429(6988):137, 2004.

[8] R.S. Coe, L. Hongre, and G. Glatzmaier. An examination of simulated geomagnetic reversals from a palaeomagnetic perspective. Phil. Trans. R. Soc. Lond. A., 358:1141–1170, 2000.

[9] C. Kutzner and U.R. Christensen. Simulated geomagnetic reversals and preferred virtual geomagnetic pole paths. Geophys. J. Int., 157:1105–1118, 2004.

[10] C. Laj, A. Mazaud, R. Weeks, M. Fuller, and E. Herrero-Bervera. Geomagnetic reversal paths. Nature, 541:447, 1991.

[11] S. K. Runcorn. Polar paths in geomagnetic reversals. Nature, 356:654–656, 1992.

[12] J. Arnou, J.L. Buttles, and G.A. Neumann. Electromagnetic core-mantle coupling and paleomagnetic reversal paths. Geophys. Res. Lett., 23:2705–2708, 1996.

[13] D. Brito, J.M. Aurnou, and P.L. Olson. Can heterogeneous core mantle electromagnetic coupling control geomagnetic reversals ? Phys. Earth Planet. Int., 112:159–170, 1999.

[14] S. O. Costin and B.A. Buffett. Preferred reversal paths caused by a heterogeneous conducting layer at the base of the mantle. J. Geophys. Res., 109, 2004.

[15] P. Rochette. Rationale of geomagnetic reversals versus remanence recording processes in rocks : A critical review. Earth Planet. Sci. Lett., 98:33–39, 1990.

[16] C.G. Langereis, A.A.M. Van Hoof, and P. Rochette. Longitudinal confinement of geomagnetic reversal paths as a possible sedimentary artefact. Nature, 358:226–230, 1992.

[17] M. Prévot and P. Camps. Absence of preferred longitude sectors for poles from volcanic records of geomagnetic reversals. Nature, 366:53–57, 1993.

[18] J. J. Love. Statistical assessment of preferred transitional VGP longitudes based on palaeomagnetic lava data. Geophys. J. Int., 140(1):211–221, 2000.

[19] J-P. Valet and E. Herrero-Bervera. Some characteristics of geomagnetic reversals inferred from detailed volcanic records. C.R. Geoscience, 335:79–90, 2003.

[20] C.G. Constable. Link between geomagnetic reversal paths and secular variation of the field over the past 5 myr. Nature, 358:230–233, 1992.

[21] L. Kristjansson. Some statistical properties of palaeomagnetic directions in Icelandic lava flows. Geophys. J. R. astr. Soc., 80:57–71, 1985.

[22] P. Camps, B. Henry, M. Prévot, and L. Faynot. Geomagnetic paleosecular variation recorded in Plio-Pleistocene volcanic rocks from Possession Island (Crozet Archipelago, southern Indian Ocean. J. Geophys. Res., 106(B2):1961–1972, 2001.

[23] C.G. Constable and C.L. Johnson. Anisotropic paleosecular variation models: Implications for geomagnetic field observables. Phys. Earth Planet. Int., 115:35–51, 1999.

[24] C. Carvallo, P. Camps, G. Ruffet, B. Henry, and T. Poidras. Mono Lake or Laschamp geomagnetic event recorded from lava flows in Amsterdam Island (southeastern Indian Ocean). Geophys. J. Int., 154:767–782, 2003.

[25] G. Plenier, P. Camps, B. Henry, and K. Nicolaysen. Paleomagnetic study of Oligocene (24-30 Ma) lava flows from the Kerguelen Archipelago (southern Indian Ocean) : Directional analysis and magnetostratigraphy. Phys. Earth Planet. Int., 133:127–146, 2002.

[26] B. Henry and C. Plessard. New palaeomagnetic results from the Kerguelen Islands. Geophys. J. Int., 128(1):73–83, 1997.

[27] J. Nougier. Terres Australes et Antarctique françaises (T.A.A.F.), Kerguelen Islands reconnaissance map, 1:200 000. Instit. Geograph. Nat'l., Paris, 1970.

[28] S. Doucet, J.S. Scoates, D. Weis, and A. Giret. Constraining the components of the Kerguelen mantle plume: A Hf-Pb-Sr-Nd isotopic study of picrites and hight-MgO basalts from the Kerguelen Archipelago. Geochem. Geophys. Geosyst., 6(4), 2005.

[29] F.A. Frey, D. Weis, H.-J. Yang, K. Nicolaysen, H. Leyrit, and A. Giret. Temporal geochemical trends in Kerguelen Archipelago basalts: evidence for decreasing magma supply from the Kerguelen plume. Chem. Geol., 164:61–80, 2000.

[30] K. Nicolaysen, F.A. Frey, K.V. Hodges, D. Weis, and A. Giret. $^{40}Ar/^{39}Ar$ geochronology of flood basalts from the Kerguelen Archipelago, southern Indian Ocean: implications for cenozoic eruption rates of the Kerguelen plume. Earth Planet. Sci. Letts., 174:313–328, 2000.

[31] S. Doucet, D. Weis, J.S. Scoates, K. Nicolaysen, F.A. Frey, and A. Giret. The depleted mantle component in Kerguelen Archipelago basalts: Petrogenesis of tholeiitic-transitional basalts from the Loranchet Peninsula. J. Petrol., 43:1341–1366, 2002.

[32] B. Henry, G. Plenier, and P. Camps. Post-emplacement tilting of lava flows inferred from magnetic study: example of Oligocene lavas in the Jeanne d'Arc peninsula (Kerguelen Islands). J. Volcanol. Geotherm. Res., 127:153–164, 2003.

[33] G. Plenier, P. Camps, B. Henry, and B. Ildefonse. Determination of flow directions by combining ams and thin-section analyses: implications for Oligocene volcanism in the Kerguelen Archipelago (southern Indian Ocean). Geophys. J. Int., 160:63–78, 2005.

[34] M.E. Derder, C. Plessard, and L Daly. Mise en évidence d'une transition de polarité du champ magnétique terrestre dans les basaltes Miocènes des îles Kerguelen. C. R. Acad. Sci. Paris, 310:1401–1407, 1990.

[35] N.D. Watkins, B.M. Gunn, J. Nougier, and A.K. Baksi. Kerguelen: continental fragment or oceanic island? Geol. Soc. Am. Bull., 85:201–212, 1974.

[36] H.-J. Yang, F.A. Frey, D. Weis, A. Giret, D. Pyle, and G. Michon. Petrogenesis of the flood basalts forming the northern Kerguelen Archipelago: Implications for the Kerguelen plume. J. Petrol., 39(4):711–748, 1998.

[37] J.L. Kirschvink. The least-squares line and plane and the analysis of paleomagnetic data. Geophys. J. R. astr. Soc., 62:699–718, 1980.

[38] R. Fisher. Dispersion on a sphere. Proc. Roy. Soc. Lond., A, 217:295–305, 1953.

[39] P.W. Reiners, T.L. Spell, S. Nicolescu, and K.A. Zanetti. Zircon (u-th)/he thermochronometry: He diffusion and comparisons with 40ar/39ar dating. Geochimica et Cosmochimica Acta, 68:1857–1887, 2004.

[40] T.A. Steven, H.H. Mehnert, and J.D. Obradovich. Age of volcanic activity in the san juan mountains, colorado. U.S. Geol. Surv. Prof. Pap., 575-D:47–55, 1967.

[41] G.T. Cebula, M.J. Kunk, H.H. Mehnert, C.W. Naeser, J.D. Obradovich, and J.F. Sutter. The fish canyon tuff, a potential standard for the 40ar-39ar and fission-track dating methods. Terra Cognita, 6th Int. Conf. on Geochronology, Cosmochronology and Isotope Geology, 6:139, 1986.

[42] I. McDougall and M. Harrison, editors. Geochronology and Thermochronology by the 40Ar/39Ar Method, volume 2nd ed. Oxford University Press, 1999.

[43] I. Wendt and C. Carl. The statistical distribution of the mean squared weighted deviation. Chemical Geology, 86:275–285, 1991.

[44] P. Riisager, K.B. Knight, J.A. Baker, I. Ukstins-Peate, M. Al-Kadasi, A. Al-Subbary, and P. Renne. Paleomagnetism and Ar/Ar geochronology of Yemeni Oligocene volcanics : Implications for timing and duration of Afro-Arabian traps and geometry of the oligocene paleomagnetic field. Earth Planet. Sci. Lett., 237:647–672, 2005.

[45] S.P. Huestis and G.D. Acton. On the construction of geomagnetic timescales from non-prejudicial treatment of magnetic anomaly data from multiple ridges. Geophys. J. Int., 129(1):176–182, 1997.

[46] S.C. Cande and D.V. Kent. Revised calibration of the geomagnetic polarity timescale for the Late Cretaceous and Cenozoic. J. Geophys. Res., 100:6093–6095, 1995.

[47] P.L. McFadden, R.T. Merrill, M.W. McElhinny, and Lee Sunhee. Reversals of the Earth's magnetic field and temporal variations of the dynamo families. J. Geophys. Res., 96(B3):3923–3933, 1991.

[48] D. Vandamme. A new method to determine paleosecular variation. Phys. Earth Planet. Int., 85:131–142, 1994.

[49] L. Tauxe and D.V. Kent. A simplified statistical model for the geomagnetic field and detection of shallow bias in paleomagnetic inclinations : was the ancient magnetic field dipolar. In J.E.T. Channell, D.V. Kent, W. Lowrie, and J.G. Meert, editors, Timescale of the paleomagnetic field, AGU Monograph. American Geophysical Union, Washington DC, 2004.

[50] L. Tauxe. Paleomagnetic Principles and Practice. Kluwer, Dordrecht, 1998.

[51] P.L. McFadden and M.W. McElhinny. Classification of the reversal test in paleomagnetism. Geophys. J. Int., 103:725–729, 1990.

[52] J. Besse and V. Courtillot. Apparent and true polar wander and the geometry of the geomagnetic field over the last 200 myr. J. Geophys. Res., 107(B11), 2002.

[53] M. Prévot, E. Mattern, P. Camps, and M. Daignières. Evidence for a 20 deg tilting of the Earth's rotation axis 110 million years ago. Earth Planet. Sci. Lett., 179:517–528, 2000.

[54] J-Y. Royer, R.D. Muller, L.M. Gahagan, C.L. Mayes, D. Nurnberg, and J.G. Sclater. A global isochron chart. University of Texas Institute for Geophysics Technical report, 117:38, 1992.

[55] R.D. Muller, J-Y. Royer, and L.A. Lawver. Revised plate motion relative to the hotspots from combined Atlantic and Indian Ocean hotspot tracks. Geology, 21:275–278, 1993.

[56] J.A. Tarduno and A.V. Smirnov. Stability ofthe earth with respect to the spin axis for the last 130 million years. Earth Planet. Sci. Lett., 184:549–553, 2001.

[57] P. Rochette, E. Tamrat, G. Feraud, R. Pik, V. Courtillot, E. Ketefo, C. Coulon, C. Hofmann, D. Vandamme, and G. Yirgu. Magnetostratigraphy and timing of the Oligocene Ethiopian traps. Earth Planet. Sci. Lett., 164:497–510, 1998.

[58] R.L. Wilson and J.M. Ade-Hall. Paleomagnetic indications of a permament aspect of the non-dipole field. In S.K.Runcorn, editor, Palaeogeophysics, pages 307–312. Academic Press, New York and London, 1970.

[59] M.W. McElhinny, P.L. McFadden, and R.T. Merrill. The time-averaged paleomagnetic field 0-5 ma. J. Geophys. Res., 101(B11):25,007–25,027, 1996.

[60] J. Carlut and V. Courtillot. How complex is the time-averaged geomagnetic field over the past 5 myr ? Geophys. J. Int., 134:527–544, 1998.

[61] N.I. Fisher, editor. Statistical analysis of circular data. Cambridge University Press, 1993.

[62] K.V. Mardia, editor. Statistics of directional data. Academic Press, 1972.

[63] J.L. Le Mouël. Outer-core geostrophic flow and secular variation of Earth's geomagnetic field. Nature, 311:734–735, 1984.

[64] G. Plenier, P. Camps, R.S. Coe, and M. Perrin. Absolute palaeointensity of Oligocene (28-30 ma) lava flows from the Kerguelen Archipelago (southern Indian Ocean). Geophys. J. Int., 154:877–890, 2003.

[65] K. Hoffman, B.S. Singer, P. Camps, L.N. Hansen, K. Johnson, S. Clipperton, and C. Carvallo. Stability of mantle control over dynamo flux since the mid-cenozoic. Nature, submitted, 2006.

[66] J.D.A. Piper and A. Richardson. The palaeomagnetism of the Gulf of Guinea volcanic province, West Africa. Geophys. J. Roy. Astron. Soc., 29:147–171, 1972.

[67] T. Kidane, B. Abebe, V. Courtillot, and E. Herrero-Bervera. New paleomagnetic result from the Ethiopian flood basalts in the Abbay (Blue Nile) and Kessem Gorges. Earth Planet. Sci. Lett., 203:353–367, 2002.

	Normal Polarity	Reversed Polarity	All
N	144	89	233
Mean Latitude	85.1	-85.8	85.5
Mean Longitude	177.6	31.5	189.3
A_{95}	3.0	3.8	2.3
R	135.23	83.73	218.91
K	16.3	16.7	16.5

Table 1: Statistical analysis of flow-average data. N is the number of lava flows, A_{95} is the 95% confidence limit about means in degrees, R is the vector sum of N unit vectors and K the Fisher concentration parameter (N-1)/(N-R).

[68] M.W. McElhinny, B.J.J. Embleton, and P. Wellman. A synthesis of Australian Cenozoic paleomagnetic results. Geophys. J. Roy. Astron. Soc, 36:141–151, 1974.

[69] J.T. Hagstrum, D.P. Cox, and R.J. Miller. Structural reinterpretation of the Ajo Mining District, Pima County, Arizona, based on paleomagnetic and geochronologic studies. Econ. Geol., 82:1348–1361, 1987.

[70] J.F. Diehl, K.M. McClannahan, and T.J. Bornhorts. Paleomagnetic results from the Mogollon-Datil volcanic field, southwestern New Mexico, and a refined mid-tertiary reference pole for North America. J. Geophys. Res., 93:4869–4879, 1988.

[71] M.E. Beck, S.D. Sherif, J.F. Diehl, E.A. Hailwood, and R.W. Lipman. Further paleomagnetic results for the San Juan Volcanic field of southern Colorado. Earth Planet. Sci. Lett., 37:124–130, 1977.

[72] A. Cox. Confidence limits for the precision parameter k. Geophys. J. R. astr. Soc., 18:545–549, 1969.

Study	Age (Ma)	Paleomagnetic pole N	Plat	Plong	Finite rotation pole λ	ϕ	ω	Rotated pole Plat	Plong	Ref
Antarctica										
1. Kerguelen	27±3	233	85.5	189.3	80.83	8.10	-3.38	85.5	179.2	This
Africa										
2. Principe volc.	24±4	25	82.8	96.6	47.14	316.10	-5.17	80.1	77.4	[66]
3. Yemen	29±2	48	74.2	249.1	40.77	357.02	-12.59	82.3	213.9	[44]
4. Ethiopia	30±1	76	78.7	209.4	42.86	316.69	-6.59	83.1	191.6	[67]
Australia										
5. Tweed volc.	22.5±2.5	75	77.4	290.9	26.28	31.19	-14.45	87.0	194.8	[68]
6. Liverpool	30±5	52	68.9	272.4	23.92	30.45	-19.06	79.0	210.3	[68]
North America										
7. Arizona	22.5±2.5	35	86.1	188.7	37.12	111.67	3.78	88.9	158.0	[69]
8. New Mexico	29.5±6.5	61	81.9	143.6	41.74	110.22	5.22	83.3	118.7	[70]
9. Colorado	26±4	36	85.0	114.0	39.86	110.93	4.50	84.2	80.9	[71]

Table 2: Global paleomagnetic pole positions with respect to the Indo-Atlantic hotspot reference frame. N is the number of sites, Plat, Plong are the latitude and longitude of the paleomagnetic pole. The finite rotation poles correspond to the Eulerian poles used to transfer the Paleomagnetic poles into the Indo-atlantic hotspot reference frame. They are calculated from Royer et al [54] and Muller et al [55]'s reconstructions using a global circuit through Central Africa.

	S_T	S_W	S_B	95%
Referred to				
Present geographic pole	20.65	5.34	20.55	19.3-22.0
Oligocene geographic pole	20.22	5.34	20.12	18.9-21.5
mean VGP	20.17	5.34	20.07	18.8-21.4

Table 3: Dispersion statistic of flow-average data for PSV dataset (N=233). S_T, S_W, S_B are the total, within, and between flow angular standard deviation, respectively. $\overline{n} = 7.185$. The 95% confidence limits on S_B is calculated using the table of Cox [72].

	PSV (N=233)	All data (N=258)
Kuiper's statistic, Cv = 1.747		
Referred to		
present geographic pole	2.610	2.545
mean Kerguelen VGP	1.297	1.077
Rayleigh's statistics, Cv = 5.991		
Referred to mean VGP	6.710	4.657

Table 4: Statistical tests of azimuthal uniformity for VGP longitudes. Cv corresponds to the critical values at the 95% significance level. When the test-statistics exceed the critical value, the hypothesis of uniformity may be rejected in favor of the alternative tested hypothesis, accepting 5% of chances to be mistaken.

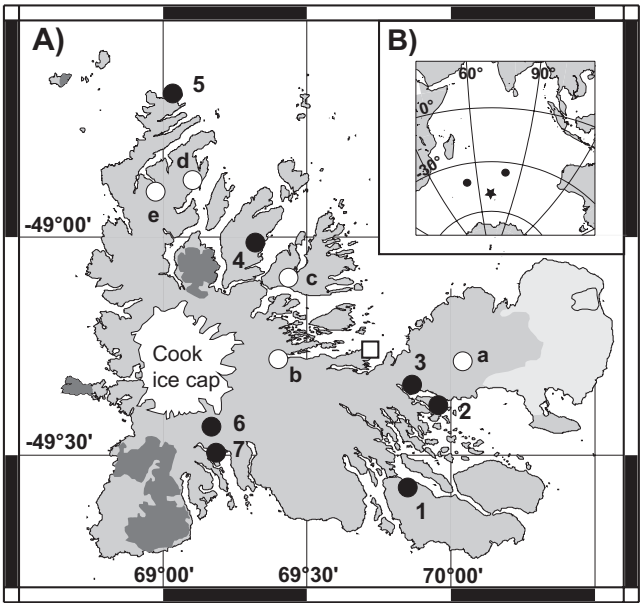

Figure 1: A/ Location of the sampling sites on a Kerguelen archipelago map. Black circles this study : (1) Port Jeanne d'Arc, (2) Ile Haute, (3) Port Raymond, (4) Mont Bureau, (5) Port Christmas, (6) Trois Ménestrels and (7) Sentinelles. Open circles [25] : (a) Mont Amery, (b) Mont Tourmente, (c) Mont Rabouillère, (d) Mont Tempête and (e) Mont des Ruches. Open Square : Port Couvreux [26]. The distributions of quaternary deposits (light grey), flood basalts (medium grey) and plutonic complexes (dark grey) are also shown. B/ Location in the Indian Ocean of the Kerguelen Archipelago (black star), Crozet Archipelago and New-Amsterdam (black circles)

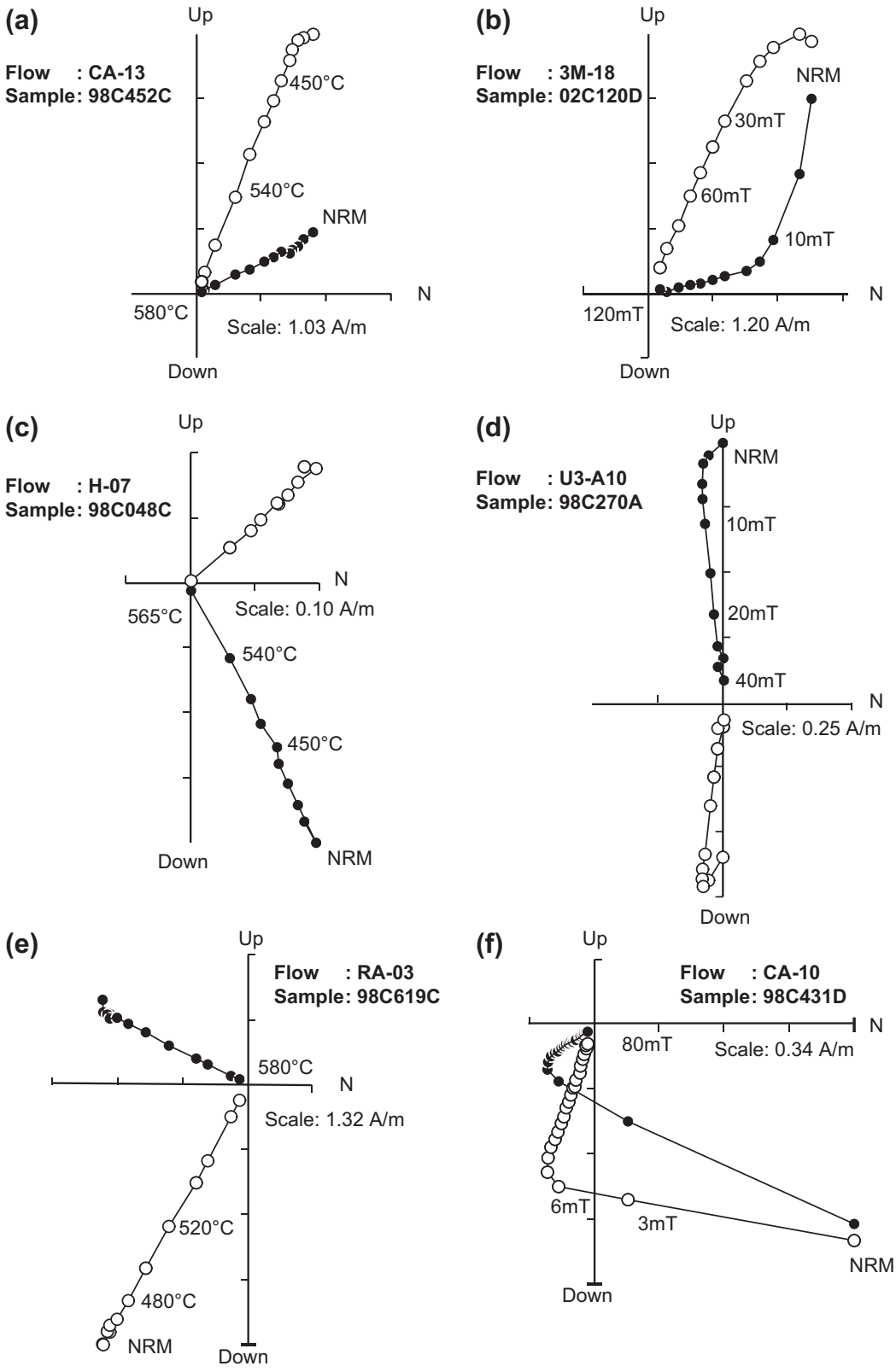

Figure 2: Example of vector endpoint diagrams of progressive thermal (left) and AF (right) demagnetizations for normal (a,b), intermediate (c,d), and reverse (e,f) directions. Projection are in geographic (a,c,e,f) or tilt corrected (b,d) coordinates. Solid (open) symbols represent projection into horizontal (vertical) planes. These diagrams show that the ChRM are easily isolated even when large secondary components are present (b,d,f).

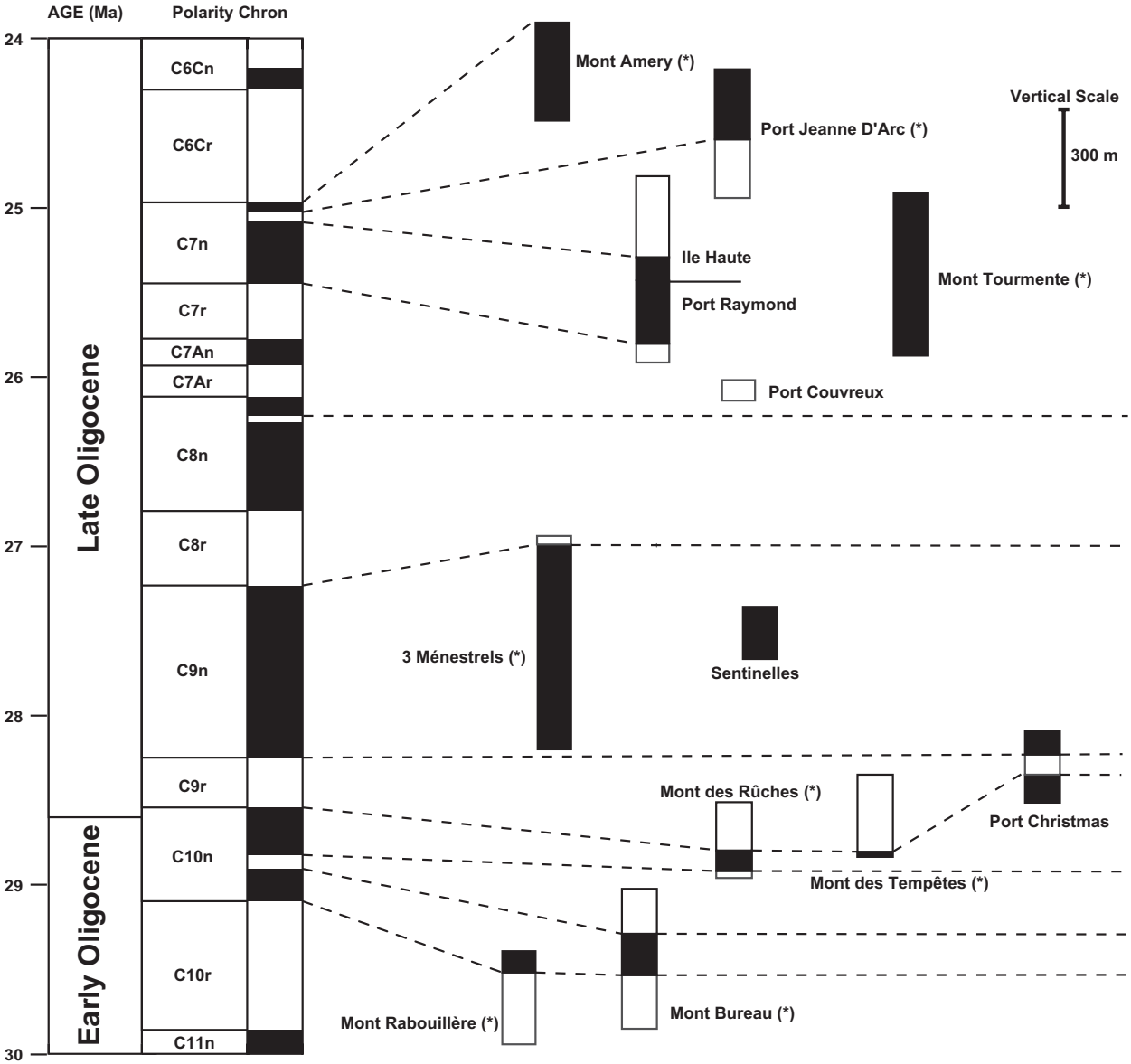

Figure 3: Magnetostratigraphic correlations with the global geomagnetic polarity time scale [45]. The sections for which radiometric ages are available are marked with an asterisk (*). We used geological and geochemical observations to correlate the remaining sections.

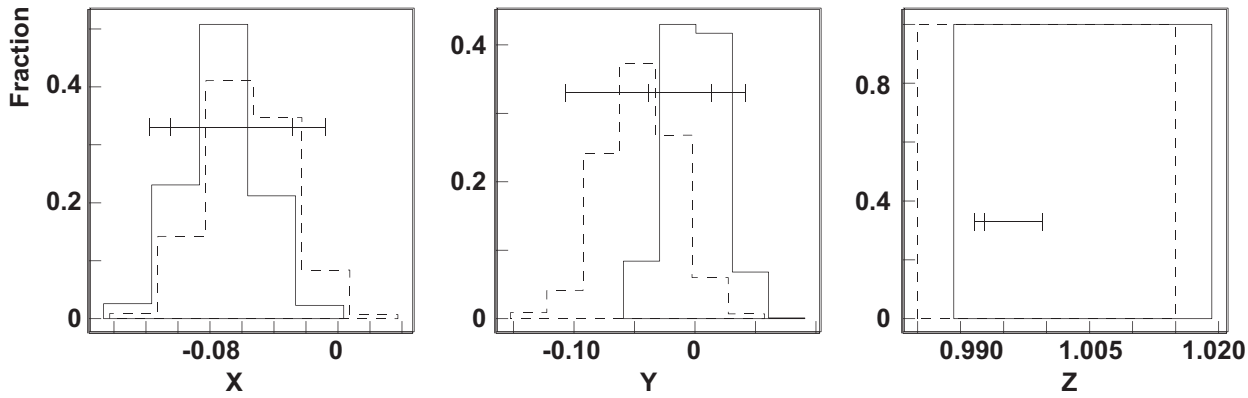

Figure 4: Histograms of cartesian coordinates of the mean bootstrapped normal (solid line) and reverse (dashed line) VGP and their 95% confidence intervals [50] for the PSV dataset (N = 233). In order to directly compare the two distributions, VGPs of reversed polarity have been flipped to their antipode. The two means cannot be distinguished at the 95% level of confidence since the confidence intervals for the two distributions overlap for each cartesian coordinate.

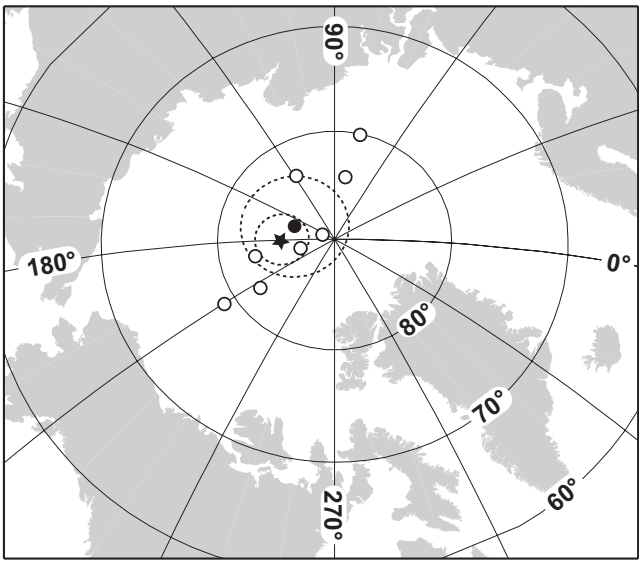

Figure 5: Selected paleomagnetic pole positions with respect to the Indo-Atlantic hotspot reference frame for the 25-30 Ma time interval (open circles) and their average (black circle) compared with the Kerguelen pole (black star). Dashed lines are the 95% confidence limit for the mean poles calculated assuming a Fisherian distribution.

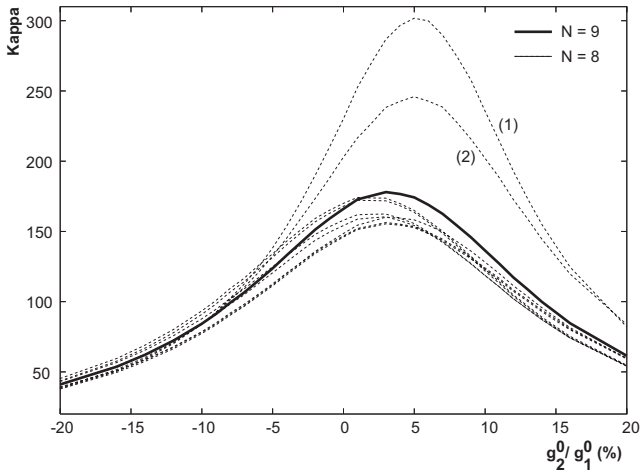

Figure 6: Fisher concentration parameter (κ) computed for the oligocene poles represented in the Indo-Atlantic hotspot reference frame. The poles locations have been recalculated for various quadrupole (g_2^0) dipole (g_1^0) field ratio. The bold curve is computed for the 9 selected poles listed in Table 2. The 9 curves in dashed lines are obtained for subset of 8 poles, one different pole being removed in turn. Maximum values for Kappa are found for a quadrupole/dipole field ratio of 5% when the Principe volcanic pole (1) or when the Liverpool volcano pole (2) are removed (2).

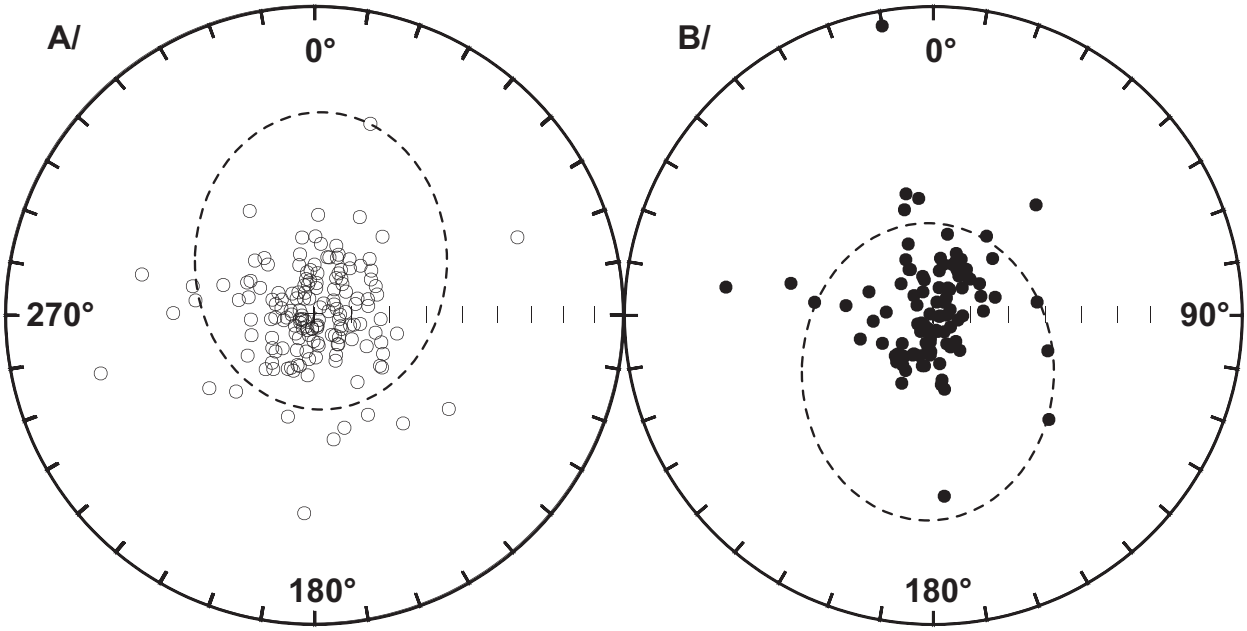

Figure 7: Whole dataset (N=258) for the Kerguelen local field directions with negative (A) and positive (B) inclinations plotted on equal area diagrams. For the both diagrams, the data have been rotated to the mean normal field direction calculated from the mean paleomagnetic pole. The dashed lines are the threshold for the Inclinations and Declinations which give VGP location at an angular distance larger than 45 $^\circ$ from the mean pole axis.

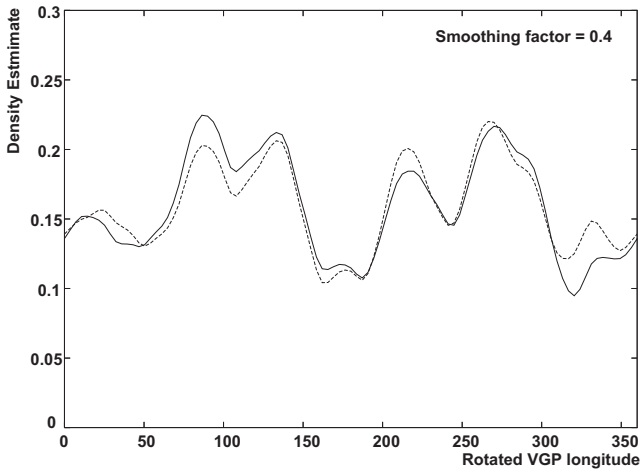

Figure 8: Non parametric density estimates calculated by means of a quartic kernel function for VGP longitude rotated in the paleomagnetic pole ($\lambda = 85.5^\circ$, ϕ= 189.3 $^\circ$) reference frame for the whole dataset N=258 (solid line) and the PSV dataset N=233 (dashed line).

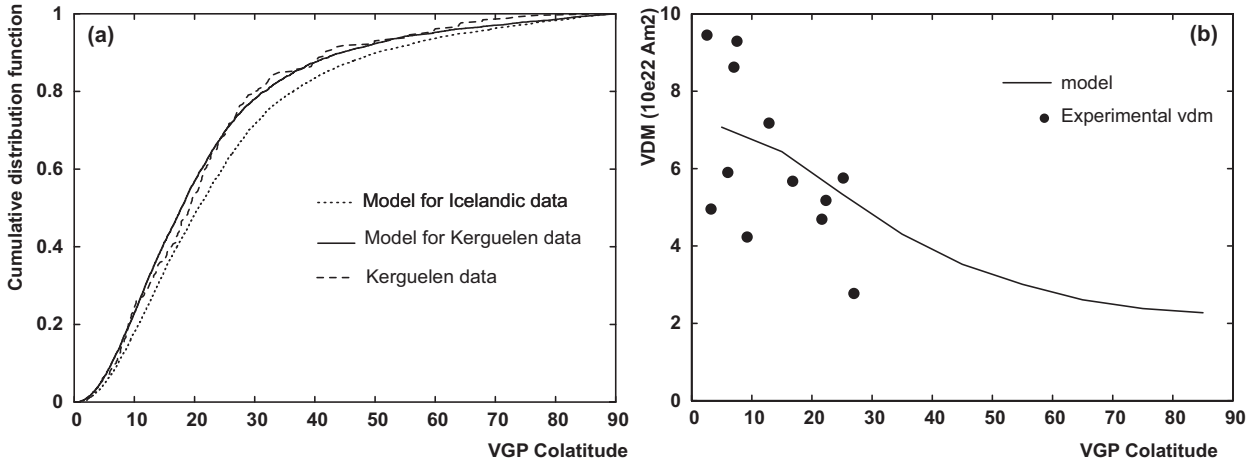

Figure 9: Data and Camps and Prevot [1]'s statistical model for the Kerguelen data set. The model is adjusted from the VGP colatitudes only, using the parameter ($\sigma^2_{AD} = 0.2$, $\sigma^2_{SV} = 0.029$) see Camps and Prevot [1] for a detailed description of the model. (a) Cumulative distribution for the VGP colatitudes, VGPs of reverse polarity being flipped to their antipodes (b) The VDMs (black circles) obtained for Kerguelen lava flows [64] are compared to the model outcomes, assuming in the model a value of $7\text{x}10^{22}$ Am^2 for the mean Axial Dipole moment. This value corresponds to the mean experimental VDM for VGPs of colatitude lower than 10°.